

# Numerical Solutions to the Time-Independent 1-D Schrödinger Equation

Danny Bennett

December 15, 2015

## Abstract

Using the Numerov algorithm, the Schrödinger equation was solved for the square well, harmonic and linear potentials. The wavefunctions were integrated using the Numerov algorithm, which required an initial trial energy, so a function was written to determine the eigenstates of the potential, allowing the numerical solutions to be obtained without any knowledge of the analytic solutions. The uncertainty relation was verified in the case of the square well and harmonic potentials, and it was observed that for large eigenstates, the harmonic potential behaves like the square well potential. The matrix Numerov algorithm was then used to solve the Schrödinger equation in a much more elegant manner.

## 1 Introduction and Theory

The aim of this experiment was to find numerical solutions to the Schrödinger equation. It was numerically solved for potentials for which the analytic solutions are well-known (infinite square well and harmonic potentials) in order to investigate the efficiency of the solutions. The wavefunctions were found and normalised, the eigenstates were determined and the uncertainty relation was verified. Finally, the 'matrix Numerov method' was used as a more elegant method of solving the Schrödinger equation for linear and harmonic potentials.

### 1.1 The Schrödinger Equation

The Schrödinger equation is a second order differential equation used in quantum mechanics to determine the wavefunctions and eigenstates of a system. It is typically of the form

$$\left(-\frac{\hbar^2}{2m} \frac{d^2}{dx^2} + V(x)\right) \Psi_n(x) = E_n \Psi_n(x), \quad (1)$$

where  $\Psi_n(x)$  are the wavefunctions,  $E_n$  are the eigenstates and  $V(x)$  is some potential. For simplicity, the particle will be contained in an infinite well, obtained by the boundary conditions:  $V(0) = V(L) = \infty$ , where  $L$  is the length of the well. It is difficult (but not impossible![3]) to solve (1) for an arbitrary potential. The most well known analytic solutions to (1) are in the cases of the square well and harmonic potentials. They shall be used in this experiment, as the known analytic solutions can provide useful insight to the validity of the numerical solutions.

It is convenient to work with a dimensionless form of (1) in order to avoid working with factors of  $\hbar$ . It can be re-written as

$$\frac{d^2}{d\tilde{x}^2} \Psi(\tilde{x}) + \gamma^2 (\epsilon - \nu(\tilde{x})) \Psi(\tilde{x}) = 0, \quad (2)$$

where  $\tilde{x} = \frac{x}{L}$  is a dimensionless distance which ranges from 0 to 1,  $\epsilon = \frac{E}{V_0}$  and  $\nu(\tilde{x}) = \frac{V(\tilde{x})}{V_0}$  are the dimensionless eigenstates and potential, where  $V_0$  is the depth of the well, and  $\gamma^2 = \frac{2mL^2V_0}{\hbar^2}$  is a dimensionless factor which accounts for the constants in the equation.

## 1.2 The Numerov Algorithm

Since (2) is of the form

$$\frac{d^2}{dx^2} \Psi(x) + k^2(x) \Psi(x) = 0, \quad (3)$$

where  $k^2(x) = \gamma^2(\epsilon - \nu(\tilde{x}))$  in this case, it can be integrated using the Numerov algorithm. By defining  $\tilde{x}$  with a discrete set of  $N$  points, separated by a distance  $l = \frac{1}{N-1}$ , (2) can be written in discrete form:

$$\frac{d^2}{d\tilde{x}^2} \Psi_n + k_n^2 \Psi_n = 0, \quad (4)$$

where  $\Psi_n \equiv \Psi(\tilde{x}_n)$ ,  $\tilde{x}_n$  being the  $n^{\text{th}}$  point, etc. The integration scheme is given by

$$\Psi_{n+1} = \frac{2\left(1 - \frac{5}{12}l^2k_n^2\right)\Psi_n - \left(1 + \frac{1}{12}l^2k_{n-1}^2\right)\Psi_{n-1}}{1 + \frac{1}{12}l^2k_{n+1}^2}. \quad (5)$$

This algorithm is obtained using Taylor expansions and the central difference method. While it could be solved using Runge-Kutta, this method takes advantage of the fact that (2) is linear in  $\Psi$  and contains only its second derivative.

## 1.3 The Matrix Numerov Method[2]

By substituting the values for  $k_n^2$  into (5), it can be written as

$$-\frac{1}{\gamma^2} \left( \frac{\Psi_{n-1} - 2\Psi_n + \Psi_{n+1}}{l^2} \right) + \frac{\nu_{n-1}\Psi_{n-1} + 10\nu_n\Psi_n + \nu_{n+1}\Psi_{n+1}}{12} = \epsilon \left( \frac{\Psi_{n-1} + 10\Psi_n + \Psi_{n+1}}{12} \right). \quad (6)$$

This can be written in matrix form by defining the following:

$$\Psi = \begin{bmatrix} \Psi_1 \\ \vdots \\ \Psi_N \end{bmatrix} \quad (7)$$

$$A = \frac{1}{l^2} (\mathbb{I}_{-1} - 2\mathbb{I}_0 + \mathbb{I}_1) \quad (8)$$

$$B = \frac{1}{12} (\mathbb{I}_{-1} + 10\mathbb{I}_0 + \mathbb{I}_1) \quad (9)$$

$$\nu = \begin{bmatrix} \nu_1 & \cdots & 0 \\ \vdots & \ddots & \vdots \\ 0 & \cdots & \nu_N \end{bmatrix} \quad (10)$$

where  $\mathbb{I}_m$  is a matrix with ones on the  $m^{\text{th}}$  diagonal and zeros elsewhere. Thus, (5) becomes

$$\left( -\frac{1}{\gamma^2} B^{-1} A + \nu \right) \Psi = \epsilon \Psi. \quad (11)$$

The operator on the left hand side clearly resembles the Hamiltonian operator (the first term being the kinetic energy operator). Therefore, the eigenvalues of this matrix will give the energies of the system. Implementing the boundary conditions  $\Psi_0 = \Psi_{N+1} = 0$  corresponds to taking  $N \times N$  submatrices of  $A$  and  $B$ .

## 2 Method

- Solutions to the dimensionless Schrödinger equation were obtained by solving the differential equation. A general solution to the differential equation was obtained and then normalisation and boundary conditions were implemented to find the normalised wavefunctions for the square well potential. The eigenstates were also determined in terms of the constant factor,  $\gamma^2$ .
- The Numerov algorithm was then implemented to find numerical solutions to the dimensionless Schrödinger equation. The first value of the wavefunction was taken to be 0 due to the boundary conditions, and the second was taken to be a small number close to 0. The algorithm was then implemented to find the remaining values of the wavefunction at the different points on the array. This was achieved using a function which takes the trial energy,  $\epsilon$ , and number of points,  $N$ , and returns the wavefunction,  $\Psi$ .
- The function which generates  $\Psi$  is only accurate when a trial energy close to the analytic eigenstates are used, which makes it redundant unless the eigenstates can be numerically approximated. The efficiency of the function can be seen by observing how far from 0 the wavefunction is at the last point. The fact that it should be 0 on the boundary was used to determine the eigenstate. This was achieved using a simple function: The value of  $\Psi_N$  at a trial energy,  $\epsilon$ , was compared to the value of  $\Psi_N$  at an updated trial energy,  $\Delta\epsilon$ . If there is a sign difference between the two wavefunctions, then the trial energy was changed by too great an amount, and it is then updated by  $-\frac{\Delta\epsilon}{2}$ . This process is repeated until  $\Psi_N$  is sufficiently close to 0, and the eigenstate is returned.
- The wavefunctions and eigenstates were determined numerically for the square well potential, but the wavefunctions were unnormalised. The wavefunctions are determined up to a constant, and this constant is fixed by demanding that  $\int_0^1 |\Psi|^2 dx = 1$ . The integration is performed numerically using Simpson's rule, and the function was updated to return the normalised wavefunctions.
- The uncertainty relation,  $\Delta\tilde{x}\Delta\tilde{p} \geq \frac{1}{2}$  in the dimensionless units, was verified for the first 10 eigenstates. The first two moments of  $|\Psi_n|^2$  were calculated and the uncertainty in position was obtained using  $\Delta\tilde{x} = \sqrt{\langle x^2 \rangle - \langle x \rangle^2}$ . The uncertainty in momentum was obtained similarly. In stationary states where the wavefunction is real,  $\langle p \rangle = 0$  and the uncertainty reduces to  $\Delta\tilde{p} = \sqrt{\langle \tilde{p}^2 \rangle}$ .
- The Schrödinger equation was then solved for a harmonic potential. The code which was previously used to solve the for the square well potential was used after a few small updates. The values of  $k_n^2$  are no longer constant, so they were stored in an array, and the function for finding the wavefunction was updated accordingly. The method of picking the trial energies in the for loop for finding the eigenstates was also updated, as the analytic solution for the previous case was no longer applicable. The energy difference between two eigenstates was plotted on a log-log scale for the first 20 eigenstates, and behaviour for higher states was investigated.
- The matrix numerov method was then used to solve the harmonic oscillator and the linear potential. Some maximum energy,  $\epsilon_m$ , was chosen, the turning points,  $x_0$  of the potential were determined (the points where  $\nu = \epsilon_m$ ); from this and some suitable region,  $\Delta x$ , outside the classically allowed region, the number of points,  $N$ , in the array was determined. The Hamiltonian matrix was obtained using (11), and its eigenstates were obtained. The numerical answers were then compared to the analytic answers.

### 3 Results and Analysis

#### 3.1 Analytic Solution to the Square Well

The analytic solution to the equation

$$\Psi'' + k^2\Psi = 0, \tag{12}$$

where  $k^2 = \gamma^2(\epsilon - \nu)$ , is required. From the form of (12), it is clear that the solution will be of complex exponential form, so it is reasonable to make the ansatz

$$\Psi(\tilde{x}) = A \sin(k\tilde{x}) + B \cos(k\tilde{x}) \tag{13}$$

for the wavefunction,  $\Psi$ . The constants can be fixed by implementing the boundary conditions and normalisation. The boundary conditions can be implemented by demanding that  $\Psi(0) = \Psi(L) = 0$ . Thus, (13) reduces to

$$\Psi_n(\tilde{x}) = A \sin(n\pi\tilde{x}), \tag{14}$$

and  $A$  can be determined by normalisation:

$$\int_0^1 |\Psi_n(\tilde{x})|^2 d\tilde{x} = 1, \tag{15}$$

which yields  $A = \sqrt{2}$ . So the analytic solution to the Schrödinger equation for the square well potential is

$$\Psi_n(\tilde{x}) = \sqrt{2} \sin(n\pi\tilde{x}), \tag{16}$$

$$\epsilon = \frac{n^2\pi^2}{\gamma^2} - 1, \tag{17}$$

since  $k = n\pi$ .

#### 3.2 Numerical Solution to the Square Well

A function was written to numerically obtain the wavefunctions for the square well potential. For a given trial energy and number of points, it iteratively updates the entries in the wavefunction array, given the first two. The function and the parameters used can be seen below. This function was used to numerically

```
15 # PARAMETERS #
16
17 N = 1000 # number of iterations
18 Psi = np.zeros(N) # wave function, start as empty array
19 g2 = 200 # gamma squared
20 v = (-1)*np.ones(N) # potential array
21 ep = -0.9 # trial energy
22 k2 = g2*(ep - v) # k squared
23 l2 = (1.0/(N-1))**2 #l squared
24
25 def wavefunction(ep, N): # finds wavefunction
26     Psi[0] = 0 # set first two values of psi
27     Psi[1] = 1e-4
28
29     for i in range(2,N): # numerov algorithm
30         Psi[i] = (2*(1-(5.0/12)*l2*k2[i-1])*Psi[i-1]
31                 -(1+(1.0/12)*l2*k2[i-2])*Psi[i-2])/(1+(1.0/12)*l2*k2[i])
32     return Psi
33
34 wavefunction(ep,N)
```

Figure 1: The function to numerically find the wavefunctions for the square well potential.

approximate the first wavefunction. A trial energy was entered, and the resulting wavefunction is shown below.

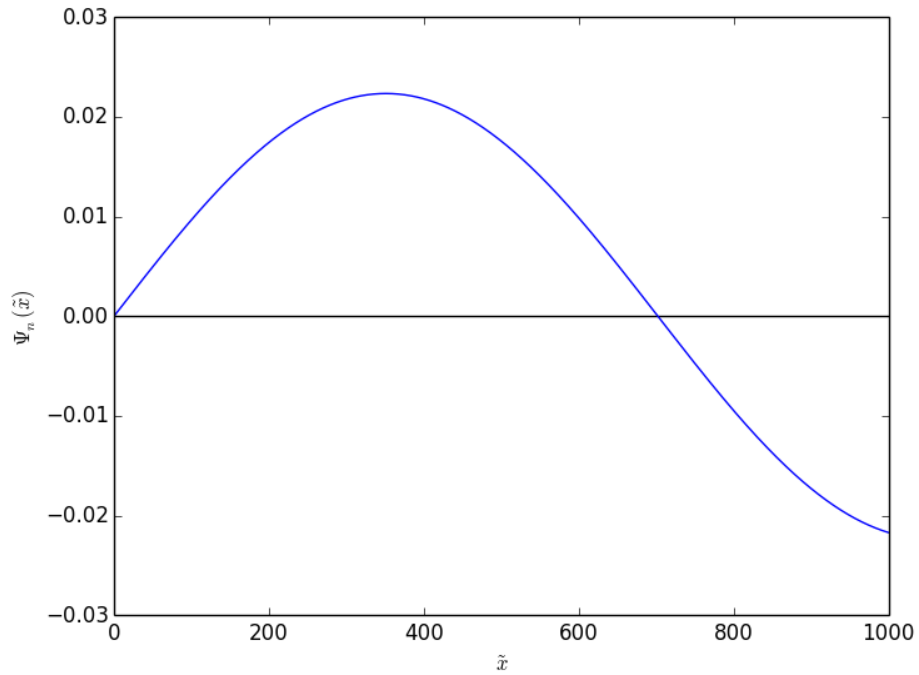


Figure 2: The numerical approximation to the first wavefunction for the square well potential. In this case the trial energy used was  $\epsilon = -0.9$ , and  $N = 1000$ .

It is clear that the boundary conditions are not fulfilled as the wavefunction does not return to 0 at the last point, meaning that the trial energy used was inaccurate. By trial and error, the trial energy can be adjusted until the end point is sufficiently close to 0 and a more accurate approximation to the wavefunction can be obtained. This defeats the purpose of numerically approximating the wavefunction however, as knowledge of the analytic solutions is required to do so efficiently. This motivates a function to determine the eigenstates numerically, as it would allow the wavefunctions to be obtained with minimal trial and error / knowledge of the analytic solutions. The function to approximate the eigenstates is shown below.

```

34 # function to find eigenstates
35 def epsilon(eps, deps, N): # takes trial energy, change in energy, N
36     k2 = g2*(eps - v) # updates k each time
37     wavefunction(Psi,k2,N)
38     P1 = Psi[N-1]
39     eps = eps + deps
40
41     while abs(deps) > 1e-12: # sets accuracy of the function
42         k2 = g2*(eps - v)
43         wavefunction(Psi,k2,N)
44         P2 = Psi[N-1]
45
46         if P1*P2<0: #if there is a sign change
47             deps = -deps/2.0
48
49         eps = eps + deps
50         P1 = P2
51     return eps # returns eigenstate

```

Figure 3: The function to determine the eigenstates for the square well potential.

This function starts with a trial energy and computes  $\Psi_{n-1}$ , then computes  $\Psi_{n-1}$  for an updated energy,  $\epsilon + \Delta\epsilon$ . if there is a sign change in sign between  $\Psi_{n-1}$  in the two cases, then  $\epsilon$  was updated by too great an amount, and the change in energy is updated to  $-\frac{\Delta\epsilon}{2}$ . This process is repeated until  $\Delta\epsilon$  is sufficiently close to 0 in order to obtain the desired accuracy in the energy, and the resulting energy is returned. It can be useful to use an accurate trial energy for this function but it is not necessary. Since the energy must be greater than the depth of the potential well ( $\epsilon > -1$  in this case), the initial energy can be chosen to be close to that value, and accurate approximations to the eigenstates will be obtained without any knowledge of the analytic expression.

$\epsilon_n$	Exact	Numerical
$\epsilon_1$	-0.95065197799	-0.95065197799
$\epsilon_2$	-0.80260791197	-0.80260791198
$\epsilon_3$	-0.55586780195	-0.55586780196
$\epsilon_4$	-0.21043164791	-0.21043164799
$\epsilon_5$	0.233700550136	0.233700549822
$\epsilon_6$	0.776528792196	0.776528791257
$\epsilon_7$	1.418053078270	1.418053075900
$\epsilon_8$	2.158273408350	2.158273403080
$\epsilon_9$	2.997189782440	2.997189771750
$\epsilon_{10}$	3.934802200540	3.934802180430

Table 1: The numerical energies compared with the exact energies

The first 10 obtained eigenstates are shown and compared with the analytic values. All of the eigenstates are correct to within 6 digit precision, although it can be seen that the first few are correct to within up to 10 digit precision. Now that the eigenstates can be accurately determined numerically, the wavefunctions can also be accurately determined. The above eigenstates were used to find the first 10 wavefunctions, and the result is shown below.

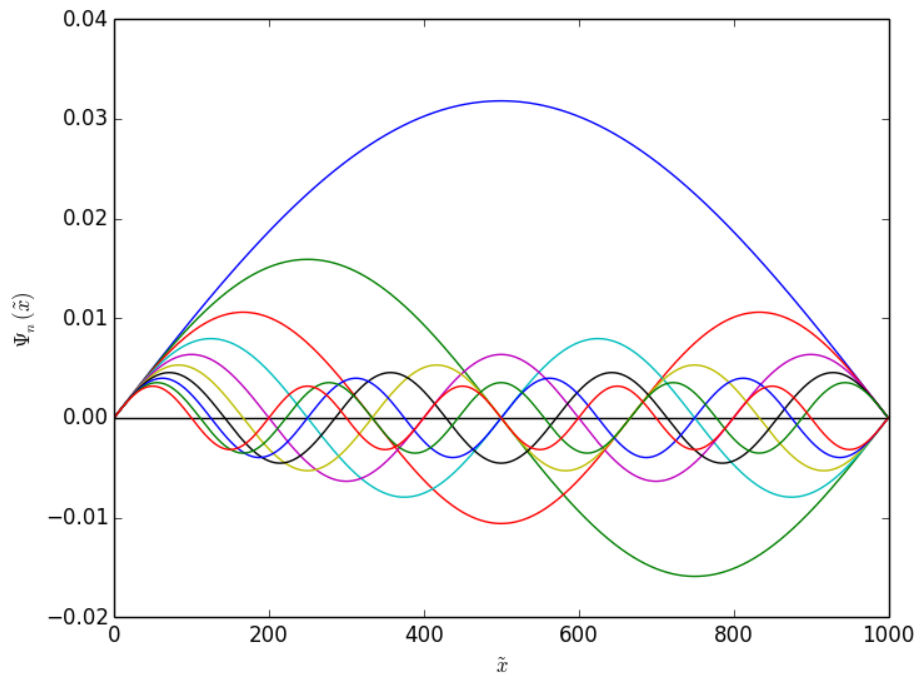


Figure 4: The first 10 wavefunctions for the square well potential.

The wavefunctions are still unnormalised. They can be normalised using a simple function, as shown below. The first normalised wavefunction was compared with the analytic solution.

```

52 def normal(Psi): # normalise Psi
53     Psi2 = Psi**2
54     I =.simps(Psi2, dx=1)

```

Figure 5: A simple function to normalise the wavefunctions. Simpsons rule is used to integrate the square of the wavefunctions, and the constant is fixed from this.

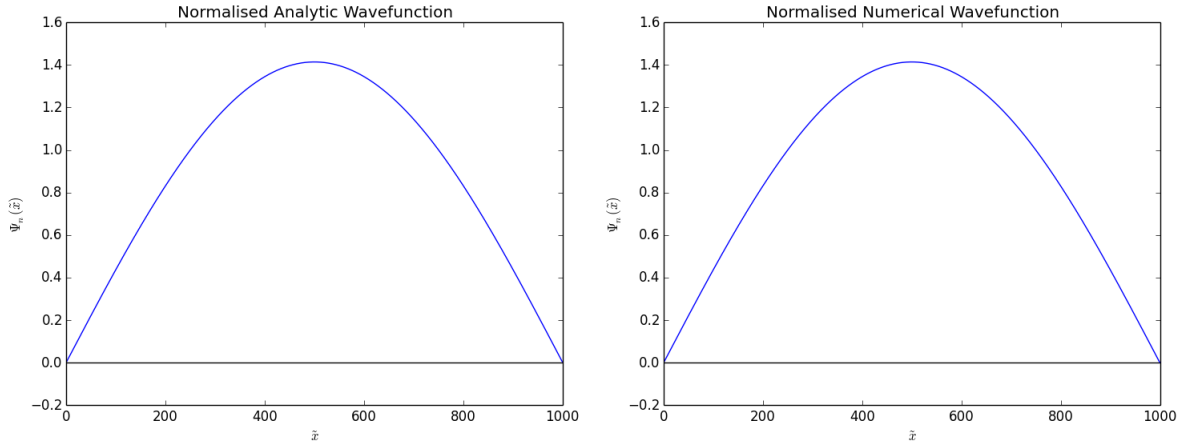


Figure 6: The numerical approximation to the first wavefunction for the square well potential agrees very well with the analytic wavefunction when normalised.

### 3.3 Verifying the Uncertainty Relation

The uncertainty relation was verified for the first 10 eigenstates. The uncertainty in position was obtained using  $\Delta\tilde{x} = \sqrt{\langle x^2 \rangle - \langle x \rangle^2}$ , where

$$\langle x^n \rangle = \int_0^1 \tilde{x}^n |\Psi(\tilde{x})|^2 d\tilde{x}. \quad (18)$$

The integrations were performed using Simpson's rule. The uncertainty in momentum ( $\tilde{p} = \frac{L}{\hbar}p$ , in dimensionless units) is given by

$$\Delta\tilde{p} = \sqrt{-\int_0^1 \Psi \frac{d^2\Psi}{d\tilde{x}^2} d\tilde{x}}. \quad (19)$$

Since the momentum operator is given by  $\tilde{p} = -i\frac{d}{d\tilde{x}}$  in this case, the moments of  $\tilde{p}$  are given by  $\langle \tilde{p}^n \rangle = i^n \int_0^1 \Psi \Psi^{(n)} d\tilde{x}$ . In the case of stationary states with real wavefunctions,  $\langle \tilde{p} \rangle = 0$ , since

$$\langle \tilde{p} \rangle = -i \int_0^1 \Psi \Psi' d\tilde{x} = -\frac{i}{2} \Psi''|_0^1 = \frac{i}{2} (k^2(1) \Psi(1) - k^2(0) \Psi(0)) = 0. \quad (20)$$

Therefore, the uncertainty in momentum is given by (19). Since this involves the second derivative of the wavefunction, an algorithm must be implemented to numerically integrate it. This is obtained using

$$\Psi''_n = \frac{\Psi_{n+1} - 2\Psi_n + \Psi_{n-1}}{l^2}, \quad (21)$$

and  $\Delta\tilde{p}$  is numerically obtained. The product  $\Delta\tilde{x}\Delta\tilde{p}$  was obtained for each eigenstate and the uncertainty relation was verified in each case. Shown below are the results for the first 10 eigenstates; it is clear that the uncertainty relation applies in every case.

$\epsilon_n$	$\Delta\tilde{x}\Delta\tilde{p}$
$\epsilon_1$	0.5672937190
$\epsilon_2$	1.6686168229
$\epsilon_3$	2.6245676131
$\epsilon_4$	3.5544340002
$\epsilon_5$	4.4745014751
$\epsilon_6$	5.3897838408
$\epsilon_7$	6.3023592156
$\epsilon_8$	7.2132478307
$\epsilon_9$	8.1230097144
$\epsilon_{10}$	9.0319777713

Table 2:  $\Delta\tilde{x}\Delta\tilde{p}$  for the first 10 eigenstates of the square well potential.

### 3.4 Harmonic Potential

The potential was changed to the harmonic potential:  $\nu(\tilde{x}) = 8(\tilde{x} - 0.5)^2 - 1$ , the eigenstates were found and the uncertainty relation was investigated in this case. The same functions as before were used to solve the harmonic potential; the only difference in this case being that  $k_n^2$  is not constant for all values of  $n$  anymore.  $k_n^2$  was defined as an array and the Numerov algorithm was updated accordingly.

$\epsilon_n$	Numerical	$\Delta\tilde{x}\Delta\tilde{p}$
$\epsilon_1$	-0.91064672344	0.49949720596
$\epsilon_2$	-0.73194016302	1.49848606872
$\epsilon_3$	-0.55323345914	2.49746455399
$\epsilon_4$	-0.37452503905	3.49644145205
$\epsilon_5$	-0.01699188364	5.49500155884
$\epsilon_6$	0.162223039646	6.49659293585
$\epsilon_7$	0.342853802917	7.50430688371
$\epsilon_8$	0.527253859604	8.52240698733
$\epsilon_9$	0.719356608827	9.54560761988
$\epsilon_{10}$	0.923857716342	10.5541671970

Table 3: The numerical energies and the uncertainty relations for the harmonic potential.

The uncertainty relation is satisfied except for the first eigenstate, although it is correct to within 1% error. This error could be due to errors made when integrating and differentiating the wavefunctions, as well as rounding errors made by the computer. A plot of  $\epsilon_n$  vs.  $n$  shows that the eigenvalues are approximately linear. This is a good sign, as the eigenvalues for the harmonic oscillator are linear in  $n$ :  $E_n = \hbar\omega(n + \frac{1}{2})$ .

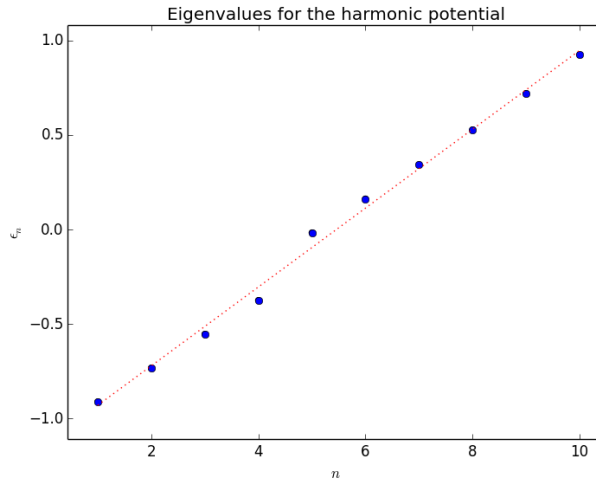


Figure 7: The eigenvalues  $\epsilon_n$  as a function of  $n$  for the harmonic oscillator.

The energy difference between successive eigenstates was obtained for the first 20 eigenstates and is plotted on a log-log scale. It is clear that for smaller eigenstates, the log of the energy difference is 0, implying that  $\epsilon_n$  varies linearly with  $n$ , which agrees with the theory. For the larger eigenstates, there appears to be an  $n^2$  dependence, which suggests that for larger energies, the harmonic potential behaves like the finite square well potential.

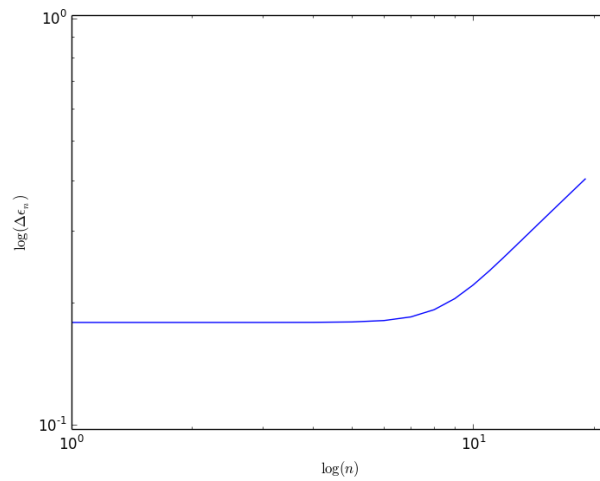


Figure 8: The energy difference,  $\Delta\epsilon_n = \epsilon_n - \epsilon_{n-1}$  for the first 20 eigenstates of the harmonic potential.

### 3.5 Using the Matrix Numerov Method

The matrix numerov method was used to solve the harmonic oscillator,  $\nu(\tilde{x}) = \frac{1}{2}\tilde{x}^2$ , and the linear potential,  $\nu(\tilde{x}) = |\tilde{x}|$ . Mathematica was used to solve these potentials due to its ability to easily manipulate large matrices. The potential was defined as a diagonal matrix, and the kinetic energy matrix was determined using (11). The number of points in the array was determined using the turning points,  $x_0$ , of the potential,  $\nu$ , and the chosen maximum energy,  $\epsilon_m$ . A suitable distance,  $\Delta\tilde{x}$ , outside the classically allowed region also contributed to the number of points to increase the accuracy of the method. Making the ansatz

$$\Psi = A \exp\left(\frac{i}{\hbar} \int \sqrt{2m(\epsilon - \nu)} d\tilde{x}\right) \quad (22)$$

for the wave function, and making a linear approximation about the turning point yields

$$\Psi = A \exp\left(-\frac{1}{\hbar} \int \sqrt{2m\nu'(\tilde{x}_0)}(\tilde{x} - \tilde{x}_0) d\tilde{x}\right). \quad (23)$$

Integrating gives

$$\Psi = A \exp\left(-\frac{2}{3\hbar} \sqrt{2m\nu'(\tilde{x}_0)} \Delta\tilde{x}^{3/2}\right), \quad (24)$$

where  $\Delta\tilde{x} = (\tilde{x} - \tilde{x}_0)$ . This ansatz describes exponential decay outside of the classically allowed region, so a good approximation for  $\Delta\tilde{x}$  can be made using the condition  $\Delta\tilde{x} \gg 1$ . This gives

$$\Delta\tilde{x} = \left(\frac{3\hbar}{\sqrt{8m\nu'(\tilde{x}_0)}}\right)^{2/3}. \quad (25)$$

The Mathematica code used to solve the harmonic oscillator is shown below. The numerical eigenstates compare very well with the exact eigenstates ( $\epsilon_n = n + \frac{1}{2}$ , in dimensionless units), and it is clear that this method is extremely effective in solving the Schrödinger equation for a given potential.

The code was then used to solve the linear potential, for which an analytic solution also exists. The analytic solution to the linear potential is given in terms of the Airy function,  $Ai(\tilde{x})$ . Defining  $a_i$  as the set of all zeros of the Airy function and  $a'_i$  as the set of all zeros of its derivative, then the expressions for the allowed even and odd energies, respectively, are given by:

$$E_n = \begin{cases} -a'_{(n+1)/2} \left(\frac{\hbar^2}{2m}\right)^{1/3} & n \text{ odd} \\ -a_{n/2} \left(\frac{\hbar^2}{2m}\right)^{1/3} & n \text{ even} \end{cases} \quad (26)$$

The eigenstates of the linear potential were obtained numerically and compared to the analytic values. The  $n = 20$  wavefunction was also obtained numerically and compared with the analytic wavefunction.

```

In[10]:= (*Potential and max energy*)
V[x_] := 0.5 x^2; ε_m = 100.;
(*Determine grid*)

x_0 = FindRoot[V[x] == ε_m, {s, ε_m}][[1, 2]]; d =  $\frac{1}{2 \sqrt{2 \epsilon_m}}$ ; Δx =  $\left(\frac{3}{\sqrt{8 V'[x_0]}}\right)^{\frac{2}{3}}$ ;

n = Round[2 (  $\frac{x_0}{d} + 10 \Delta x$  )]; x = Table[-  $\frac{d (n+1)}{2} + d i$ , {i, n}];

(*Kinetic Energy Matrix*)
I[n_, d_] := DiagonalMatrix[1 + 0 Range[n - Abs[d]], d];
B =  $\frac{1}{12}$  (I[n, -1] + 10 I[n, 0] + I[n, 1]);
A =  $\frac{1}{d^2}$  (I[n, -1] - 2 I[n, 0] + I[n, 1]);
KE =  $\frac{-1}{2}$  Inverse[B].A;

(*Hamiltonian*)
H = KE + DiagonalMatrix[V[x]];
(*Energies wavefunctions*)
Reverse[Eigenvalues[H, -10]]

Out[18]= {0.5, 1.5, 2.5, 3.5, 4.5, 5.5, 6.5, 7.5, 8.49999, 9.49999}

```

Figure 9: A simple piece of Mathematica code to implement the matrix Numerov method.  $\epsilon_m$  is some maximum energy and hence the minimum deBroglie wavelength is  $\lambda = \frac{\hbar}{\sqrt{2m\epsilon_m}}$ . The spacing between the successive points will be accurate if taken to be about one point per radian:  $d = \frac{\lambda}{2\pi}$ . The  $\Delta x$  term accounts for a sufficient distance outside of the classically allowed region. It is obtained by making a linear approximation to the WKB approximation of the wavefunction.

$\epsilon_n$	Exact	Numerical
$\epsilon_1$	0.8086165	0.8085306
$\epsilon_2$	1.8557570	1.8557570
$\epsilon_3$	2.5780961	2.5780691
$\epsilon_4$	3.2446076	3.2446075
$\epsilon_5$	3.8257152	3.8256970
$\epsilon_6$	4.3816712	4.3816711
$\epsilon_7$	4.8918202	4.8918058
$\epsilon_8$	5.3866137	5.3866135
$\epsilon_9$	5.8513009	5.8512887
$\epsilon_{10}$	6.3052630	6.3052626

Table 4: The numerical energies compared with the exact energies for the linear potential.

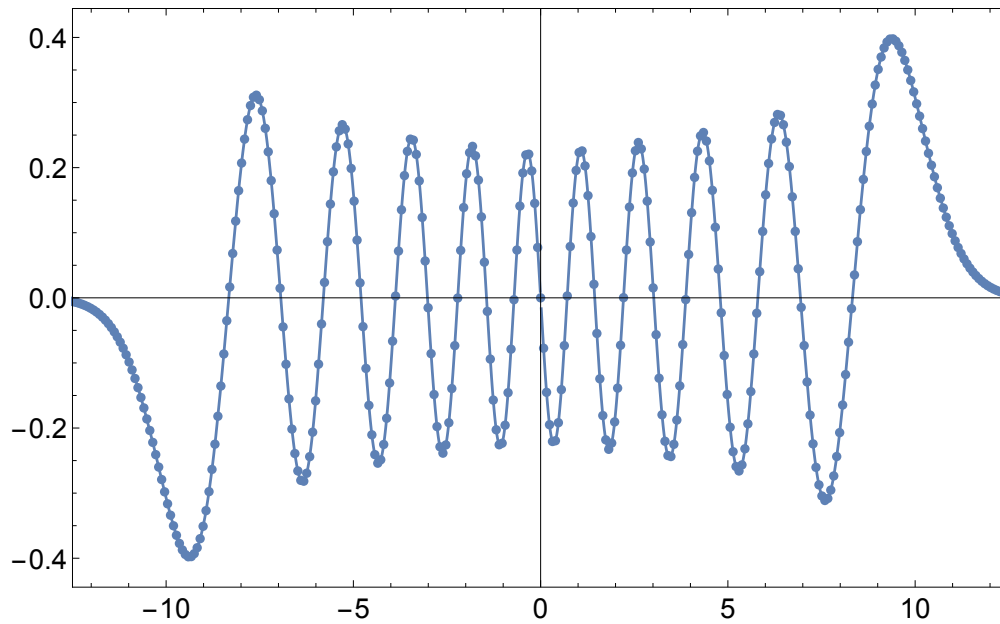


Figure 10: The  $n = 20$  wavefunction for the linear potential. The dots are the numerical solution and the curve is the analytic solution.

## 4 Discussion and Conclusions

The Schrödinger equation was successfully solved for the square well potential. The numerical wavefunctions and eigenstates both compared very well with the analytic solutions. The wavefunctions were successfully, which allowed the uncertainty relation to be investigated. It was satisfied for all eigenstates except for one, where there was a 1% error due to numerical inaccuracies. The eigenstates of the harmonic potential were obtained, and they appeared to vary linearly with  $n$ , which is a good indicator that they are accurate. From the log-log plot of the energy differences for the harmonic potential, it was observed that for the larger eigenstates, the harmonic potential behaves similarly to the square well potential.

The matrix Numerov algorithm was successfully used to solve the harmonic oscillator and the linear potential. This method is very accurate and efficient. The accuracy of the method could be improved by increasing the maximum energy (and hence the number of points,  $N$ ), although this is achieved at the cost of longer running times. One possible way to improve the accuracy of the Numerov algorithm in general is to introduce variable step sizes[1], which would reduce the number of evaluations required when compared to the standard method.

## References

- [1] Hafez Kobeissi and Majida Kobeissi. A new variable step method for the numerical integration of the one-dimensional schrödinger equation. Journal of Computational Physics, 77(2):501–512, 1988.
- [2] Mohandas Pillai, Joshua Goglio, and Thad G Walker. Matrix Numerov Method for Solving Schrödinger's Equation. Anthology American Journal of Physics Year: 2012, 80(1017).
- [3] A. Voros. Zeta-regularization for Exact-WKB Resolution of a General 1D Schrödinger Equation. Journal of Physics A Mathematical General, 45:K4007, September 2012.